Research Article

Journal of Physical Organic Chemistry

Received: 16 June 2008, Revised: 29 September 2008, Accepted: 3 October 2008, Published online in Wiley InterScience: 26 November 2008

(www.interscience.wiley.com) DOI 10.1002/poc.1469

A theoretical and experimental study of the polar Diels–Alder cycloaddition of cyclopentadiene with nitrobenzodifuroxan

Dmitry V. Steglenko[a], Mikhail E. Kletsky[a], Sergey V. Kurbatov[a], Artem V. Tatarov[a], Vladimir I. Minkin[a]*, Régis Goumont[b]* and François Terrier[b]*

The mechanism of the Diels–Alder interaction of 4-nitrobenzodifuroxan (NBDF) with cyclopentadiene (Cp), resulting in the highly stereoselective formation of the stable endo [2+4] adduct has been elucidated by combining density functional theory (DFT) and experimental studies. Calculations at the B3LYP/6-31G* level reveal that this adduct does not derive from a direct normal electron demand cycloaddition process. Instead, the evidence is that the interaction proceeds initially through a very polar inverse electron demand process to afford the intermediate [4+2] cycloadduct. Then, this species undergoes a complete conversion into the more stable isomeric endo [2+4] adduct via a [3+3] Claisen-type sigmatropic shift. The lifetime of the [4+2] intermediate was sufficient to allow its full ^{1}H NMR characterization at −10 °C. Viewing the results in the general context of the Diels–Alder reactivity of nitrobenzofuroxans, a noteworthy feature is that the similar behavior of NBDF and 4-aza-6-nitrobenzofuroxan (ANBF) goes along with a similar positioning of the two compounds on the general electrophilicity scale of Parr *et al*.

Supporting information may be found in the online version of this article.

Keywords: polar Diels–Alder cycloaddition; superelectrophilic olefins; nucleophile–electrophile combination; nitrobenzofuroxans; DFT calculations

INTRODUCTION

The high susceptibility of nitro-substituted 2,1,3-benzoxadiazoles and related 10-π-electron heteroaromatic substrates to undergo covalent nucleophilic addition or substitution processes has long attracted considerable attention.[1–25] Quantitative evaluation of thermodynamic reactivity for these Meisenheimer electrophiles is nicely provided by a comparison of the pK_a values for water addition. The pK_a values for hydration of the prototype 4,6-dinitrobenzofuroxan (DNBF, **1**) and 4-aza-6-nitrobenzofuroxan (ANBF, **2**) structures to yield the σ-complexes **C-1** and **C-2** are 3.75 and 4.06, respectively, in aqueous solution, as compared with a pK_a value of 13.43 for formation of the analogous adduct **C-3** of 1,3,5-trinitrobenzene (TNB, **3**).[8,26,27] Based on these figures, neutral compounds such as **1** and **2** have been accorded superelectrophilic properties.[26,27] This has led to numerous synthetic, analytical and biological applications.[10,11,28–33]

Of equal interest, however is that compounds like **1** and **2** have also been found to undergo a variety of Diels–Alder reactions, a behavior which is in itself evidence that the six-membered ring of these superelectrophilic heterocycles has a poor aromatic character relative to TNB.[26,34–39]

As illustrated in Scheme 1, DNBF can formally behave as do nitroalkenes,[40,41] being susceptible to act as a dienophile in normal electron-demand (NED) Diels–Alder reactions as well as a heterodiene in inverse electron-demand (IED) Diels–Alder reactions.[42,43] In Scheme 1, the reaction of DNBF with cyclopentadiene (Cp) affords initially a mixture of the two stereoselective NED and IED adducts, i.e. the [2+4] and [4+2] adducts **5** and **6**, respectively.[37] Because the remaining nitroolefinic fragment of the monoadduct **6** is also very reactive, diadduct formation subsequently occurs, proceeding with high stereoselectivity to give the highly functionalized structure **7** as the thermodynamically stable product of the reaction.[37] The reaction of ANBF with Cp has also been studied, yielding a mixture of the two [2+4] and [4+2] monoadducts **8** and **9** at −20 °C. Raising the temperature to 0 °C led to conversion of **9** into the more stable adduct **8** (Scheme 2).[26]

Density functional theory (DFT) calculations have been recently carried out which have fully confirmed the reactivity patterns depicted in Schemes 1 and 2.[43,44] More importantly, however, these calculations have demonstrated that the formation of the [2+4] and [4+2] DNBF adducts **5** and **6** proceeds through the initial formation of the zwitterionic

* *Correspondence to: R. Goumont, Institut Lavoisier de Versailles (ILV), UMR 8180, University of Versailles, 45 Etats-Unis Ave., 78035 Versailles Cedex, France. E-mail: goumont@chimie.uvsq.fr*

a *D. V. Steglenko, M. E. Kletsky, S. V. Kurbatov, A. V. Tatarov, V. I. Minkin*
Department of Chemistry, Southern Federal University, 7 Zorge St., 344090 Rostov-on-Don, Russian Federation

b *R. Goumont, F. Terrier*
Institut Lavoisier de Versailles (ILV), UMR 8180, University of Versailles, 45 Etats-Unis Ave., 78035 Versailles Cedex, France

Journal of Physical Organic Chemistry

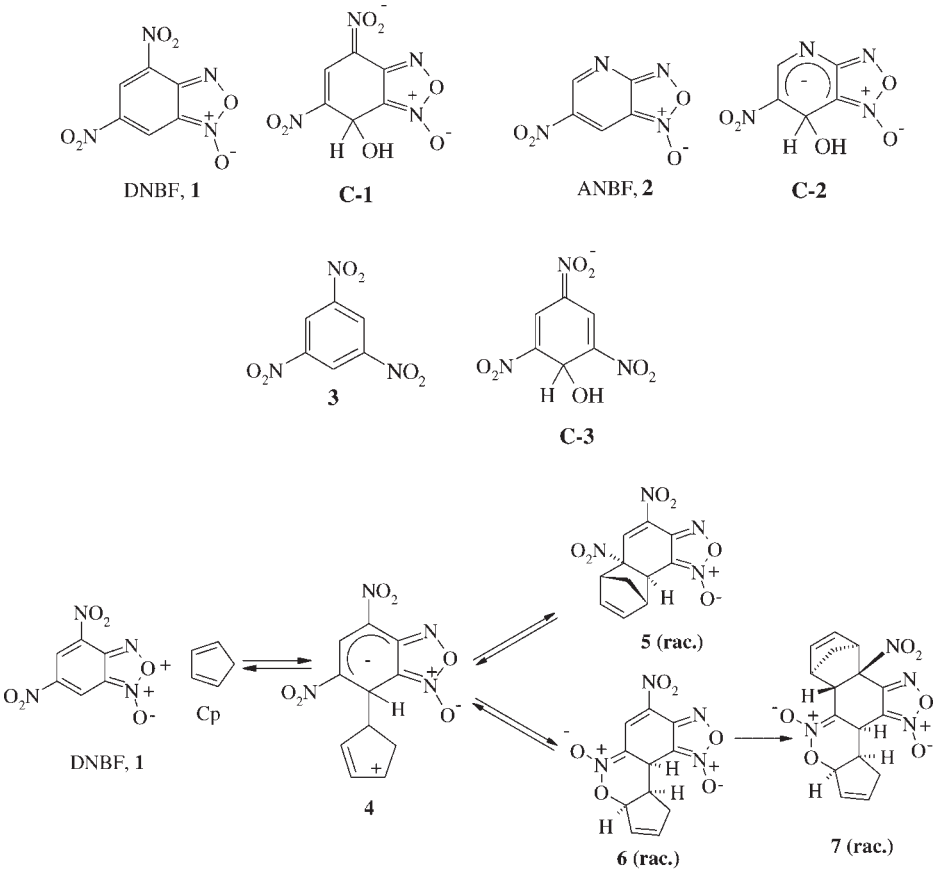

Scheme 1.

intermediate **4**.[43] Similarly, the formation of the diadduct **7** from the monoadduct **6** also involves the formation of a zwitterion. Contrasting with the results for DNBF, no zwitterionic intermediate of sufficient stability, i.e. **10**, could be identified on the reaction coordinate pertaining to the formation of the ANBF monoadducts **8** and **9**.[44] The interaction proceeds through a very polar transition state to give the [4+2] adduct **9** which is subsequently converted into the more stable [2+4] isomer **8** via a [3+3] Claisen-type sigmatropic shift.[44]

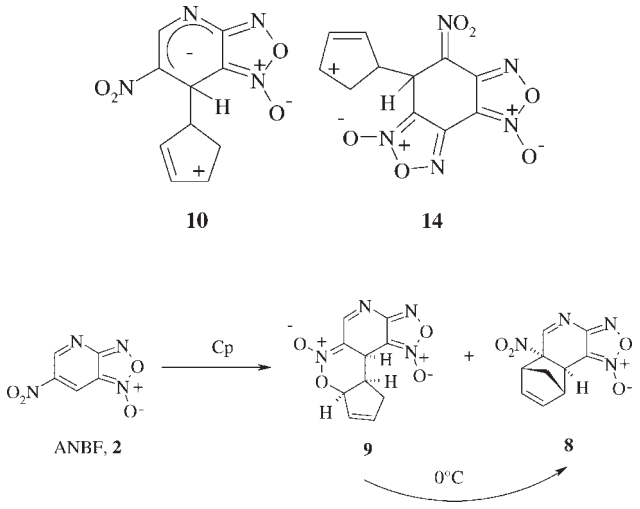

Scheme 2.

Recently, we have shown that the dual superelectrophilic and Diels–Alder reactivity extends to the single nitroolefinic fragment of the 4-nitrobenzodifuroxan (NBDF, **11**) molecule.[45,46] Thus, the reaction of NBDF with Cp proceeds very readily in chloroform to give the endo [2+4] adduct **12** whose structure has been confirmed by X-ray crystallography.[45,46] An interesting feature, however is that the nitroolefinic fragments of NBDF and ANBF have similar electrophilicities, as measured by the values of the global electrophilicity index, ω, introduced by Parr.[47] The question was therefore posed of whether the isolated NBDF adduct **12** was formed directly through either a zwitterionic intermediate, i.e. **14**, or a strongly polar transition state, or was the result of a sigmatropic rearrangement of the so far undetected [4+2] isomer **13** (Scheme 3). We report here the results of a DFT study of the NBDF/Cp system which was carried out using the same calculations strategy as that developed by Domingo *et al*. for the DNBF/Cp and ANBF/Cp systems.[43,44] Based on the results obtained, an experimental reinvestigation of the NBDF reactivity has been carried out which has allowed the NMR identification of **13** as a transient adduct along the reaction coordinate.

As recall by a referee, strong polar Diels–Alder reactions are governed by charge transfer processes and not by molecular orbital interactions, so that the use of the NED and IED terms to classify the [2+4] and [4+2] adducts identified in the present work is not conceptually correct. Referring to this formalism is useful, however, and here helpful to correlate our results with

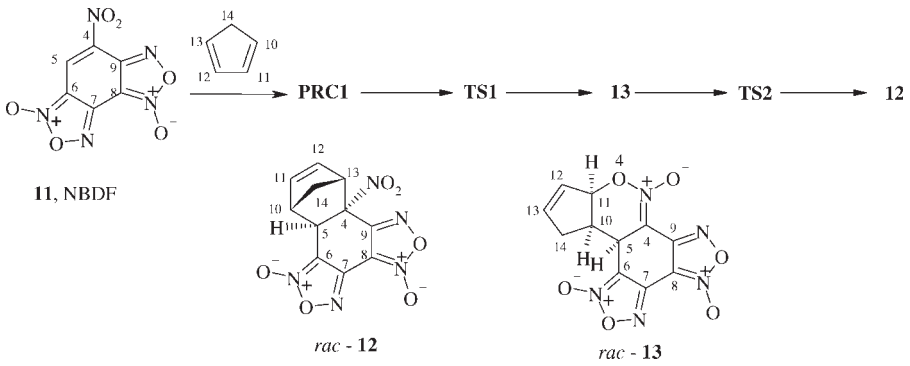

Scheme 3.

those obtained in previously reported studies of the Diels–Alder reactivity of DNBF.

RESULTS AND DISCUSSION

Computational methods and reactivity indexes

Calculations based on the method of DFT were performed using the B3LYP exchange correlation functional,[48,49] together with the standard 6-31G* basis set,[50] as developed by Domingo *et al.* for the DNBF/Cp and ANBF/Cp interactions.[44] Full geometry optimization was achieved by the Berny analytical gradient optimization method.[51,52] The stationary points were characterized by frequency calculations in order to ascertain that the transition state structures are associated with only one imaginary frequency. Minimum energy reactions paths (MERPs) were determined by gradient scanning from the transition state (TS) structures in both direct and reverse directions of the transition vector.[53] NBO (Natural Bond Orbital) analysis was performed for all stationary points.[54,55]

With dichloromethane as a reference ($\varepsilon = 8.93$), solvent effects were considered for all stationary points on the basis of the polarizable continuum model (PCM) of Tomasi *et al.*[56–59] All computations were carried out with the Gaussian 03 suite of programs.[60]

Recent studies have shown that some reactivity indexes can be defined within the DFT theory which are very useful for predicting the feasibility as well as the more or less polar character of Diels–Alder reactions.[43,44,61–63] These include the global electrophilicity index, ω, introduced by Parr and defined by Eqn 1.[47,64,65] In this equation, the electronic chemical potential μ and the chemical hardness η of a substrate are two parameters which were evaluated in terms of the one-electron energies of the frontier molecular orbitals (FMOs) ie; the Highest Occupied Molecular Orbit (HOMO) and the Lowest unoccupied Molecular Orbital (LUMO) at the ground state of the molecules: $\mu = \frac{1}{2}(\varepsilon_H + \varepsilon_L)$; $\eta = (\varepsilon_L - \varepsilon_H)$.[47,64,65] Another informative index used by Domingo *et al.* is the so called ΔN_{max} parameter, defined by Eqn (2), which is a measure of the maximum amount of electronic charge that the electrophilic partner can accept.[47] Calculated values ω, μ, η, and ΔN_{max} of relevance for our study are collected in Table 1. Also important is the local electrophilicity index (ω_k) defined by Eqn (3) which shows that the electrophilic character of a molecule will develop to the greatest extent at the site where the Fukui function for nucleophilic attacks (f_k^+) displays its maximum value, i.e. at the most reactive site of the electrophile.[63] Calculated ω_k values for NBDF are given in Fig. 1.

$$\omega = \frac{\mu^2}{2\eta} \tag{1}$$

$$\Delta N_{max} = -\frac{\mu}{\eta} \tag{2}$$

$$\omega_k = \omega f_k^+ \tag{3}$$

Global and local electrophilicity analysis

Recent investigations have used the ω values to classify dienes and dienophiles on a unique scale.[43,44,61–63,66,67] According to this model, the polar character of a Diels–Alder interaction can be assessed from the difference, $\Delta\omega$, in the global electrophilicities of the two reagents as well as the ΔN_{max} values for the system at hand. Thus, it can be safely anticipated that reactions involving a diene and a dienophile located at the ends of the ω scale will proceed with an especially strong polar character.[61–63,66] In turn, reactions associated with small $\Delta\omega$ values should be prototypes of non-polar processes.[61–63,66] At the same time, consideration of the local electrophilicity indexes has proved to be useful to account for the regioselectivity in DA (Diels-Alder) reactions exhibiting a polar character.[43,44,61–63]

With ω values $\geq$4.8, NBDF, ANBF, and DNBF correspond to the most electrophilic compounds so far ranked on the ω scale (Table 1). As a result, their reactions with Cp, and most other dienic structures, are characterized with large $\Delta\omega$ values. This leaves no doubt that the related cycloadditions will exhibit a large polar character. For comparison, it is only in the presence of a Lewis acid catalyst that the electrophilicity of nitroethylene becomes associated with a high ω value, for example $\omega = 4.33$ for the nitroethylene /BH_3 complex, making it possible to engage this attractive nitroolefin in many C—C coupling reactions, including strongly polar Diels–Alder reactions.[40–42,61–63,68–72] Similarly, appropriate Lewis acid catalysts have to be employed to enhance the electrophilicity of nitro-activated olefins such as trans-β-nitrostyrene and 1,1-dinitro-2,2-diphenylethylene as well as of cyano- and carbonyl-activated olefins, e.g. benzylidenemalonitrile, which have ω values comparable to that of nitroethylene.[73,74]

The large polar character predicted by the ω values for the Diels–Alder reactions implying DNBF, ANBF, and NBDF implies the regiochemistry of the cycloadditions be determined by the local electrophilicities, as measured by ω_k.[43,44] As a matter of fact, the

Journal of Physical Organic Chemistry

Table 1. Electronic chemical potential μ, chemical hardness η, global electrophilicity ω, and ΔN_{max} parameter for dienophiles and dienes discussed in this work[a]

Olefin-type compound	μ	η	ω	ΔN_{max}
DNBF[b]	−0.2177	0.1180	5.46	1.84
ANBF[c]	−0.2084	0.1229	4.81	1.69
NBDF[d]	−0.2144	0.1300	4.80	1.65
Nitroethylene / BH_3[e]	−0.2046	0.1316	4.33	1.55
1,1-Dinitro-2,2-diphenylethylene[f]	−0.1835	0.1439	3.16	1.27
Benzylidenemalonitrile[f]	−0.1832	0.1529	2.99	1.20
Trans-β-nitrostyrene[f]	−0.1759	0.1582	2.70	1.11
Nitroethylene[e]	−0.1958	0.2001	2.61	0.98[b]
2,3-Dimethylbutadiene[e]	−0.1211	0.2074	0.97	0.58[b]
Isoprene[e]	−0.1212	0.2120	0.94	0.57[b]
Cyclopentadiene[e]	−0.1106	0.2016	0.83	0.55[b]

[a] Electronic chemical potential μ and chemical hardness η in atomic units; global electrophilicities ω in eV as defined by Eqn 1; ΔN_{max} in electron units.
[b] Reference 43.
[c] Reference 44.
[d] This work.
[e] Reference 43.
[f] Reference 67.

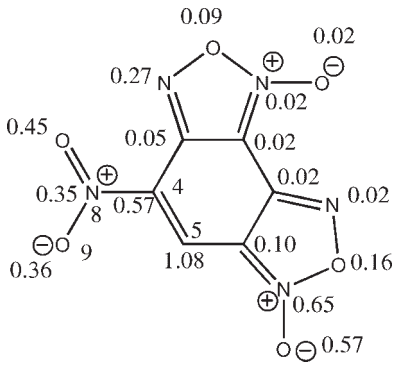

Figure 1. Local electrophilicity indices ω_k for NBDF (in eV)

reactivity patterns experimentally observed for DNBF and ANBF cycloadditions, as depicted in Schemes 1 and 2, are fully consistent with the C7 carbon being the most electrophilic center of the parent molecules.[26,37] Figure 1 shows that the unsubstituted C5 carbon of NBDF is by far associated with the greatest local electrophilicity ($\omega_k = 1.08$), implying that this position should be the preferred site for a nucleophilic addition process. As shown below, this reactivity is also in agreement with the asynchronicity found to prevail in the TS for formation of the [4+2] cycloadduct **13**.

MERP for the NBDF/Cp interaction

A thorough analysis of the gas-phase results reveals that the Diels–Alder reaction of NBDF with Cp to give the thermodynamically stable and isolable [2+4] adduct **12** consists of three steps: (1) the initial formation of a molecular complex of the charge transfer type type named PRC1, whose geometry is given in Fig. 2; (2) movement through the highly asynchronous transition state, TS1, to form the [4+2] cycloadduct **13**; (3) the conversion of **13** into the [2+4] adduct **12** through a transition state TS2 corresponding to a [3,3] sigmatropic shift. The different stationary points of the interaction are shown, together with the atom numbering, in Scheme 3 and Fig. 3. The energetic results are collected in Table 2 while the geometries of the transition states are given in Fig. 4.

B3LYP/6-31G* calculations allow the characterization of the pre-reaction complex, PRC1, whose formation is associated with a stabilization energy of 3.0 kcal/mol. Additional calculations using the basis set superposition error (BSSE) method[75,76] confirm that the formation of PRC1 corresponds to a real minimum on the potential energy surface, predicting however a lower stability (1.3 kcal/mol) for this species. Also, calculations at the B3LYP/6-311++G* level predict the formation of PRC1 with a stabilization energy of 1.7 kcal/mol. The reaction of PRC1 has also been studied through NBO analysis.[54,55] This shows that the molecular complex is of the CT type, arising from the interaction between the bonding π-molecular orbital of Cp with the antibonding σ^*-molecular orbital of the NBDF molecule. Surprisingly, previous calculations carried out at the same level of theory did not lead to the characterization of similar prereaction complexes in the DNBF/Cp and ANBF/Cp interactions.[43,44] Nevertheless, relatively stable CT-complexes have been experimentally characterized in the reactions of DNBF and NBDF with donor molecules such as naphthalene.[77]

Exploration of the MERP for the NBDF/Cp interaction allows the characterization of the transition state TS1 associated to the attack of Cp on the nitroolefinic fragment of NBDF within the prereaction complex. The activation barrier for this process which leads to the [4+2] cycloadduct **13** is 15.3 kcal/mol. As shown in Fig. 4, TS1 is a highly imbalanced transition state with the formation of the C5—C10 bond (1.931 Å) being strongly ahead of the formation of the O4—C11 bond (2.540 Å). This situation

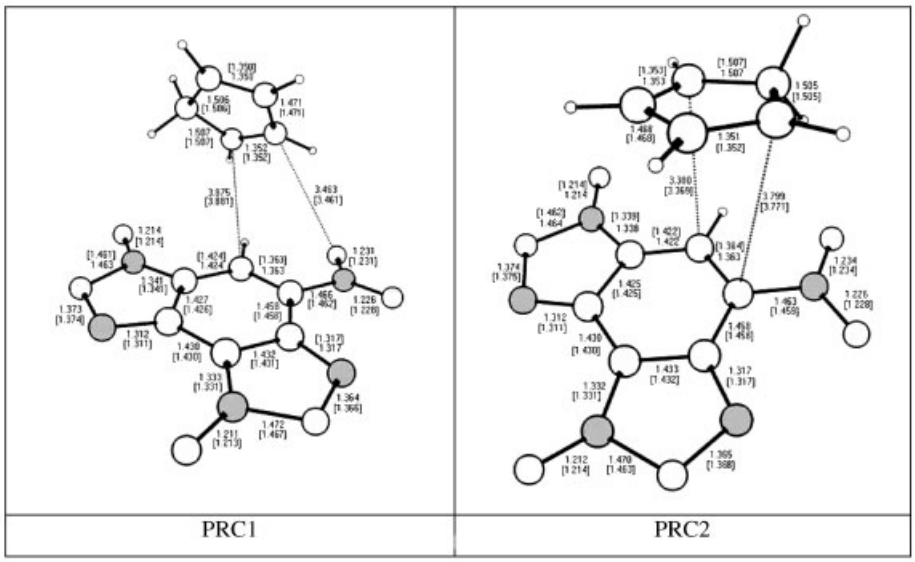

Figure 2. Main bond lengths (in Å) for pre-reaction complexes PRC1 and PRC2 identified in the reaction of NBDF with Cp in the gas phase and in dichloromethane (in square brackets)

reflects the large polar character of the cycloaddition affording the adduct **13** in which Cp is acting essentially as a nucleophile. It follows that TS1 is strongly zwitterionic in nature, even though the calculations did not provide evidence for the zwitterion **14** being an intermediate along the reaction coordinate of the interaction. A consequence of the zwitterionic character of TS1 is that the O4—C11 distance is markedly shorter than the distance between the C4 and C13 atoms (3.168 Å), due to a favorable coulombic interaction between the two former atoms. Importantly, this interaction accounts for the preferred formation of the IED adduct **13** rather than the related NED adduct **12**. It also explains the large endo selectivity observed in this polar cycloaddition.[44]

In agreement with the experimental evidence that the [2+4] cycloadduct **12** is the thermodynamically stable product of the NBDF/Cp interaction, the calculations have allowed the characterization of a transition state, TS2 corresponding to the conversion of **13** into **12** via a [3,3] sigmatropic shift. The activation barrier for this process in the gas phase is high (27 kcal/mol), perhaps due to B3LYP overestimation of the energy of the intermediate **13,** but the energy level of TS2 (11.1 kcal/mol) is lower than that of TS1 (12.3 kcal/mol). It should be mentioned that the energy barrier of transformation **12** → **13** estimated by the NMR method is 26.4 kcal/mol, i.e. it is very close to the B3LYP result. The calculations at the B3LYP/6-31G* do not properly account for the relative stabilities of the two adducts, however,

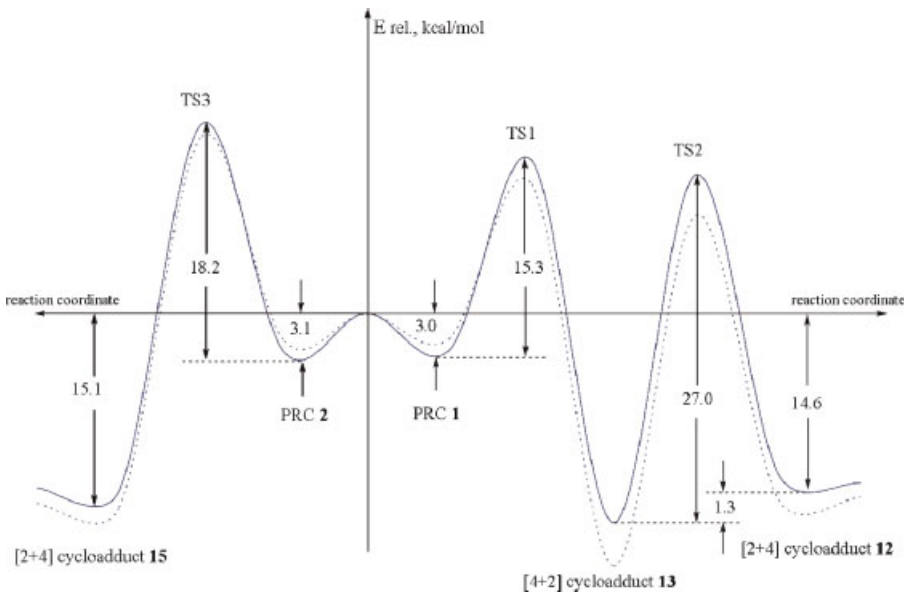

Figure 3. Energy profile for the NBDF/Cp interaction. The solid lines correspond to gas phase processes while the dotted lines correspond to reactions in dichloromethane.

Table 2. Total (*E*, in a.u.) and relative (Δ*E*, in kcal/mol)[a] energies of the stationary points of the Diels–Alder reaction between 4-nitrobenzodifuroxan (NBDF, **11**) and cylopentadiene (Cp), in the gas phase and in dichloromethane, as derived from B3LYP/6-31G* calculations

	Gas phase			Dichloromethane	
	E	Δ*E*	Δ*E*[b]	*E*[c]	Δ*E*
Cp	−194.10106	—	—	−194.10230	—
NBDF	−953.91950	—	—	−953.92753	—
PRC1	−1148.02535	−3.0	−2.6	−1148.03263	−1.8
TS1	−1148.00102	12.3	13.8	−1148.01532	9.1
13	−1148.04582	−15.9	−11.6	−1148.05800	−17.7
TS2	−1148.00292	11.1	13.6	−1148.01882	6.9
12	−1148.04384	−14.6	−10.3	−1148.05238	−14.1
PRC2	−1148.02554	−3.1	−2.6	−1148.03285	−1.9
TS3	−1147.99648	15.1	16.7	−1148.01005	12.4
15	−1148.04461	−15.1	−10.7	−1148.05351	−14.9

[a] Relative to the total energy of isolated reagents NBDF and Cp.
[b] Relative energies including the zero point energy (ZPE) correction.
[c] The SCF energy after PCM corrections.

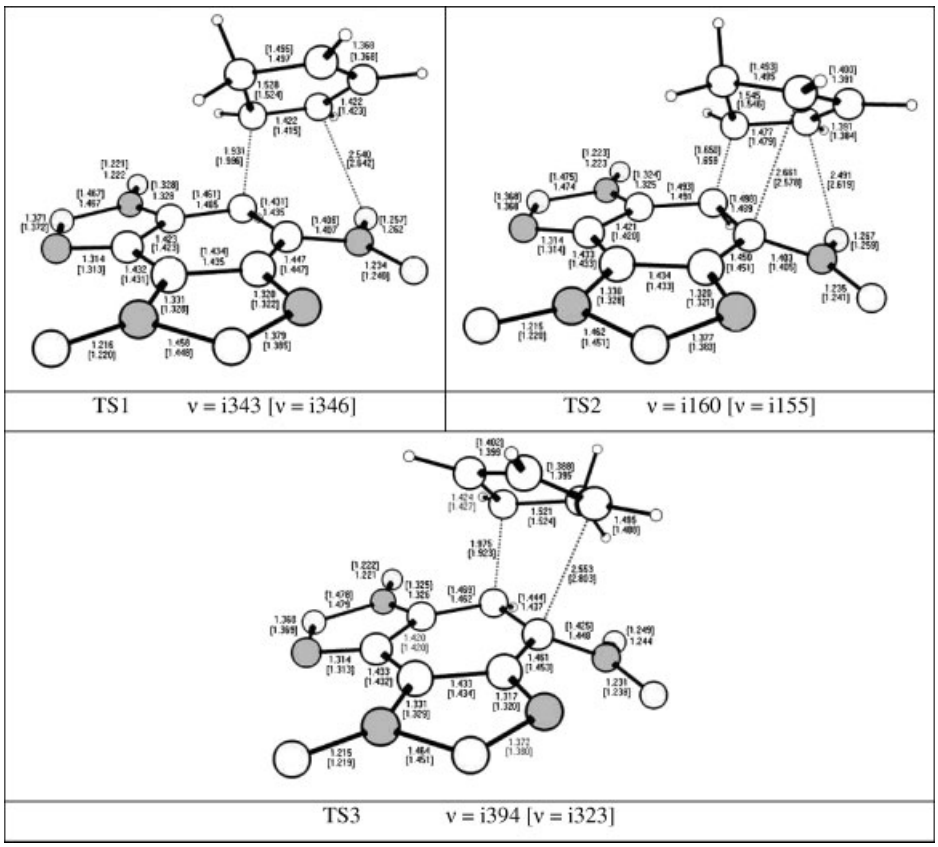

Figure 4. Main bond lengths (in Å) in the transition states pertaining to the various steps involved in the NBDF/Cp interaction (Scheme 3) in the gas phase and in dichloromethane solution (in square brackets). The unique imaginary frequencies (in cm^{-1}) are also given

Table 3. Total (E, in a.u.) and relative energies (ΔE, in kcal/mol) of the stationary points of the Diels–Alder reaction between NBDF **11** and Cp in the gas phase, as derived from *ab initio* (HF/6-31G*) calculations

	E	ΔE^a	ΔE^b
Cp	−192.79172	—	—
NBDF	−948.66478	—	—
PRC1	−1141.46103	−2.8	−2.4
TS1	−1141.41630	25.2	26.6
13	−1141.48247	−16.3	−11.3
TS2	−1141.42423	20.2	23.0
12	−1141.49060	−21.4	−16.3
PRC2	−1141.46131	−3.0	−2.6
TS3	−1141.40927	29.6	31.0
15	−1141.49241	−22.5	−17.5

[a] Relative to the sum total energy of isolated reagents.
[b] Relative energies including the zero point energy (ZPE) correction.

since they predict that the [4+2] adduct **13** is 1.3 kcal/mol more stable than the [2+4] adduct **12**. In the current DFT approach, it is not possible to estimate the error of the calculations without comparing them to other methods or experiments. We have recalculated for the gas phase all stationary points mentioned above by the HF/6-31G* method (Table 3). Going to the HF/6-31G* level reveals that **12** is in fact more stable than **13** by 5.1 kcal/mol, in full consistency with experimental observations.[44] At the same time the relative stabilities of all other structures are qualitatively analogous to DFT results in Table 2.

Two other results are noteworthy: (1) there is a rather similar development in the breaking of the O4—C11 bond (2.491 Å) and the formation of the C4—C13 bond (2.661 Å) at TS2 for the sigmatropic shift leading from **13** to **12**; (2) a X-ray structure of **12** has been made,[45,46] leaving no doubt regarding the endo selectivity of the cycloaddition. Figure 5 shows the remarkable agreement between the X-ray data and the geometrical characterization of **12**, as deduced from B3LYP/6-31G* calculations. To confirm that the endo approach is by far the preferred mode of reactivity in the NBDF/Cp interaction, calculations have been extended to the exo approach of Cp relative to the NO_2 substituent of NBDF. As shown in the left part of Fig. 3, a prereaction complex (PRC2) of the same stability as the one involved in the endo mode of reactivity is initially found. Then, only one transition state of imbalance character (TS3) corresponding to a direct formation of the exo [2+4] adduct **15** could be identified. Interestingly, the activation barrier for this polar cycloaddition is 2.9 kcal/mol higher than the one for the formation of the endo [4+2] adduct **13**. At the same time, the energy level of TS3 is 2.8 kcal/mol higher than that of TS1, in full agreement with the non-observation of **15**.

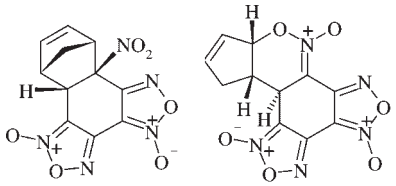

rac - **15** *rac* - **16**

The extent of the charge transfer occurring along the polar NBDF/Cp reactions has been evaluated through a NBO analysis.[54,55] The transfer of negative charge from Cp, the donor molecule, to NBDF, the acceptor molecule is 0.38e at TS1 and 0.35e

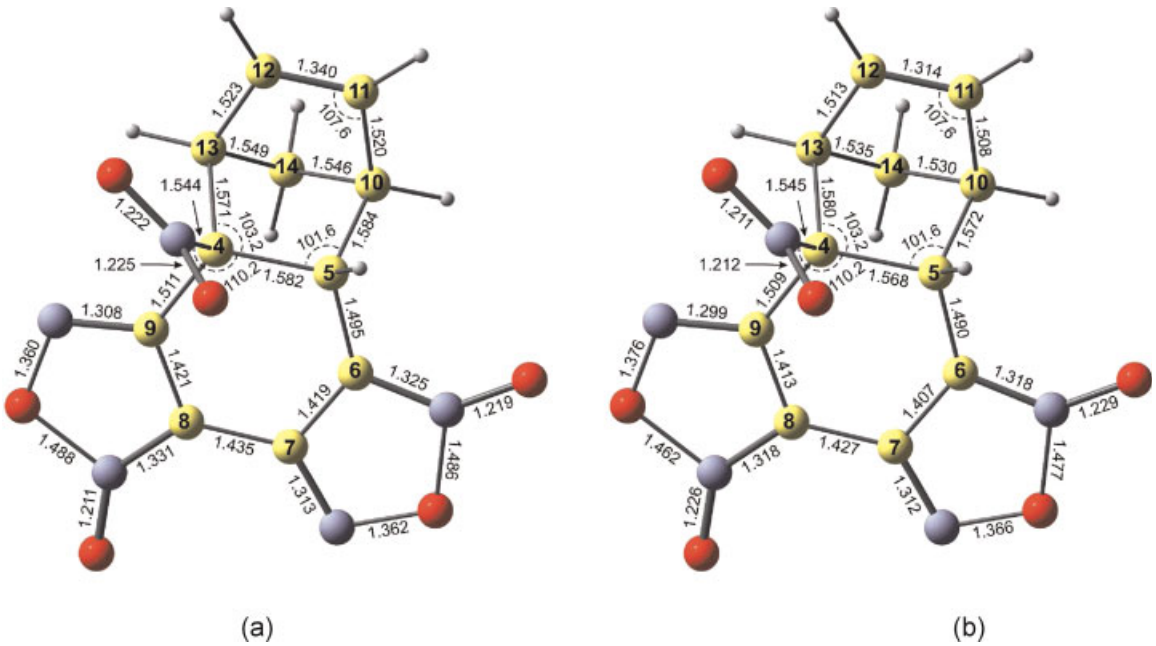

(a) (b)

Figure 5. The geometrical characteristics of the [2+4] cycloadduct **12** according to B3LYP/6-31G* calculations (a) and X-ray analysis (b). Bond lengths are given in Å and bond angles in degrees.

Journal of Physical Organic Chemistry

at TS3. This clearly supports the zwitterionic character of the transition states. Also of interest are the results of an analysis of the atomic motion at the unique imaginary frequency of TS1 (343 cm^{-1}) and TS3 (394 cm^{-1}). This analysis reveals that these two transition states are for the most part associated to the movement of the C5 and C10 atoms along the developing C5—C10 bond. The movement of other important atom sites, i.e. O4, C11, C4, and C13, is insignificant. It thus appears that the related cycloadditions proceed as simple two-center interactions. Regarding TS2, the analysis at the unique imaginary frequency of 160 cm^{-1} confirms that the breaking of the O4—C11 bond and the formation of the C4—C13 bond are essentially coupled (vide supra).

Going to dichloromethane solution does not cause significant changes in the gas phase geometries (Figs 3 and 4) while increasing markedly the stabilization of the polar transition states (Table 2). This results in lower activation barriers for the cycloadditions in CH_2Cl_2 with, however, no modification in the reactivity pattern found in the gas phase. In particular, all attempts to locate a zwitterionic intermediate and a second transition state associated to a stepwise mechanism for formation of **13** have failed.

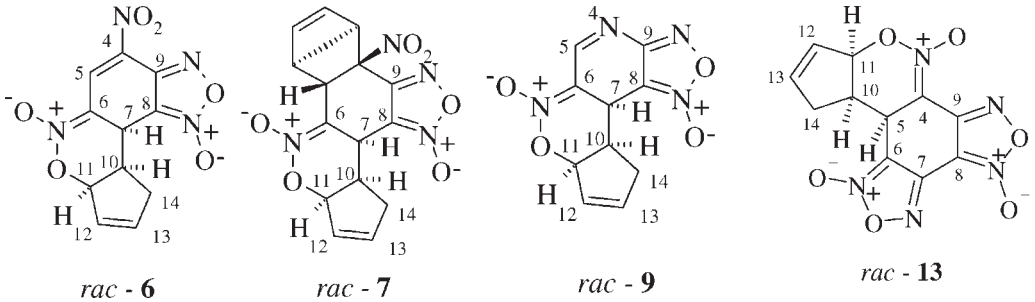

rac - **6** *rac* - **7** *rac* - **9** *rac* - **13**

Characterization of the transient [4+2] cycloadduct 13

A most significant feature which emerges from the above calculations is that the NBDF/Cp interaction proceeds via the initial formation of the IED adduct **13** in a strongly exothermic process, i.e. $\Delta E = -15.9$ kcal/mol in the gas phase. Then the conversion of **13** into the thermodynamically more stable adduct **12** occurs with a large activation barrier of 27 kcal/mol. These figures suggested that **13** should have a sufficient lifetime to be characterized by NMR under appropriate experimental conditions.

As a matter of fact, treatment of NBDF by Cp at −10 °C in acetone resulted in complex ^{1}H NMR spectra (Figure S1) consistent however, with the formation of a mixture of two products. Notably, one of these products was identical to the previously characterized NED adduct **12** in a pure form. This, as well as the progressive clarification of the spectra observed upon raising the temperature at 20 °C and shifting the interaction towards the complete formation of **12**, aids in the recognition of the various resonances assignable to the adduct **13** (Figures S1–S4). The ^{1}H NMR data for this species are given in Table 4 together with similar data previously collected for the related IED adducts of ANBF and DNBF.

As diagnostic features for structure **13** there is the presence of a doublet at $\delta = 4.72$ ppm assignable to the proton H5 and a multicoupled signal at $\delta = 4.15$ ppm typical of the proton H10. Also supporting structure **13** is the close similarity of the chemical shifts pertaining to this adduct and the related DNBF and ANBF adducts **6**, **7**, and **9**, respectively. While it is noteworthy that the IED Diels–Alder reaction leading to **13** proceeds diastereoselectively, as it does for **6**, **7**, and **9**, it should be noted that Nuclear Overhauser Effects (NOE) experiments did not allow a firm discrimination between the two diastereomeric structures **13** and **16** through NOE experiments. However, the close analogy between the $^3J_{H5H10}$ coupling constant in **13** ($^3J_{H5H10} = 5.4$ Hz) and the related $^3J_{H7H10}$ coupling constant in the DNBF adducts **6** and **7** ($^3J_{H7H10} = 5.9$ Hz) strongly supports the view that the stereochemistry firmly established for **6** and **7** (X-ray structure)[37] also holds for **13**. As a matter of fact, gas phase calculations show that **16** is both kinetically ($\Delta E = 4.1$ kcal/mol) and thermodynamically ($\Delta E = 1$ kcal/mol) less favored than **13**.

Table 4. ^{1}H NMR data for the cyclopentadiene [4+2] adducts of DNBF (**6**), ANBF (**9**), and NBDF (**13**)[a]

Compound	H_5	H_7[b] H_5[c]	H_{10}	H_{11}	H_{12}	H_{13}	H_{14}	$^3J_{H7H10}$[b] $^3J_{H5H10}$[c]
6 ($CDCl_3$)	8.33	4.32	4.13	5.89	5.92	6.24	2.59/1.96	5.9
7 ($CDCl_3$)	—	4.06	3.98	5.77	5.95	6.21	2.41/2.16	5.9
9 ($CDCl_3$)	8.66	4.26	4.01	5.92	5.92	6.17	2.57/1.97	5.6
13 (Acetone-d_6)	—	4.72	4.15	5.76	5.93	6.08	2.50/2.32	5.2

[a] δ in ppm and J in Hertz.
[b] H_7 for structures **6**, **7**, and **8**.
[c] H_5 for structure **13**.

CONCLUSION

Combining the information provided by DFT calculations and experimental studies has allowed to delineate the mechanism of the Diels–Alder interaction of NBDF with Cp to afford the [2+4] adduct **12** as the thermodynamically stable product and synthetically isolable compound. Contrasting with the results for the DNBF/Cp interaction (Scheme 1), no zwitterionic intermediate of sufficient stability could be identified on the reaction coordinate leading to the two characterized cycloadducts **12** and **13** (Scheme 3). Instead, it is found that the reactivity pattern of the NBDF/Cp system is similar to the one established for the ANBF/Cp system (Scheme 2), with the initial formation of the [4+2] adduct **13** being followed by its conversion into **12** via a [3+3] sigmatropic shift. Interestingly, the observed mechanistic differences are consistent with the positioning of the three electrophiles on the global electrophilicity scale, ω, introduced by Parr *et al*. With ω values of 4.81 and 4.80, respectively, ANBF and NBDF react similarly with Cp, exhibiting a strong electrophilicity which is not, however, sufficient to generate a zwitterionic intermediate, i.e. **10** or **14** of definite stability. Going from NBDF to DNBF strongly increases the electrophilicity, as measured by a jump of ω to 5.46. The inference of the superelec-trophilicity of DNBF is that the putative zwitterionic intermediate **4** arising from the nucleophilic addition of Cp is now stable enough to exist as a discrete entity along the reaction coordinate.

EXPERIMENTAL SECTION

Nitrobenzodifuroxan **11** was synthesized according to a procedure reported by A. S. Bailey and J. R. Case.[77]: mp 158–159 °C (lit.[78] 158 °C). Cp was obtained from the heating of bicyclopentadiene and was used without further purification. ^{1}H and ^{13}C NMR spectra were recorded on a 300 MHz spectrometer. Chemical shifts are reported in ppm (J values in Hertz) relative to internal Me_4Si.

Acknowledgements

The authors are grateful to CNRS (France) and RFBR (Russia) for providing support through a PICS (n° 3863) exchange program.

REFERENCES

[1] M. R. Crampton, *Adv. Phys. Org. Chem.* **1969**, *7*, 211–257.
[2] M. J. Strauss, *Chem. Rev.* **1970**, *70*, 667–712.
[3] F. Terrier, *Chem. Rev.* **1982**, *82*, 77–152.
[4] E. Buncel, in *The Chemistry of Amino, Nitro and Nitroso Compounds*, Vol. 2, part 2 (Ed.: S. Patai), Wiley, London, **1982**, 1225; Supplement F.
[5] E. Buncel, M. R. Crampton, M. J. Strauss, F. Terrier, in *Electron-Deficient Aromatic and Heteroaromatic-Base Interactions*, Elsevier, Amsterdam, **1984**.
[6] F. Terrier, in *Nucleophilic Aromatic Displacement. The Influence of the Nitro Group*, (Ed.: H. Feuer), VCH, New York, **1991**.
[7] A. Gasco, A. J. Boulton, *Adv. Heterocycl. Chem.* **1981**, *29*, 251–340.
[8] F. Terrier, F. Millot, W. P. Norris, *J. Am. Chem. Soc.* **1976**, *98*, 5883–5890.
[9] F. Terrier, A. P. Chatrousse, Y. Soudais, M. Hlaibi, *J. Org. Chem.* **1984**, *49*, 4176–4181.
[10] F. Terrier, E. Kizilian, J. C. Halle, E. Buncel, *J. Am. Chem. Soc.* **1992**, *114*, 1740–1742.
[11] F. Terrier, M. J. Pouet, J. C. Halle, S. Hunt, J. R. Jones, E. Buncel, *J. Chem. Soc. Perkin Trans. 2* **1993**, 1665–1672.
[12] M. J. Strauss, R. A. Renfrow, E. Buncel, *J. Am. Chem. Soc.* **1983**, *105*, 2473–2474.
[13] E. Buncel, R. A. Renfrow, M. J. Strauss, *J. Org. Chem.* **1987**, *52*, 488–495.
[14] R. A. Manderville, E. Buncel, *J. Chem. Soc. Perkin Trans. 2* **1993**, 1887–1898.
[15] E. Buncel, R. A. Manderville, J. M. Dust, *J. Chem. Soc. Perkin Trans. 2* **1997**, 1019–1026.
[16] M. R. Crampton, L. C. Rabbitt, *J. Chem. Soc. Perkin Trans. 2* **1999**, 1669–1674.
[17] M. R. Crampton, L. C. Rabbitt, F. Terrier, *Can. J. Chem.* **1999**, *77*, 639–646.
[18] M. R. Crampton, L. C. Rabbitt, *J. Chem. Soc. Perkin Trans. 2* **2000**, 2159–2166.
[19] M. R. Crampton, R. A. Lunn, D. Lucas, *Org. Biomol. Chem.* **2003**, *1*, 3438–3443.
[20] C. Boga, E. Del Vecchio, L. Forlani, A. Mazzanti, P. E. Todesco, *Angew. Chem. Int. Ed.* **2005**, *44*, 3285–3289.
[21] L. Forlani, A. L. Tocke, E. Del Vecchio, S. Lakhdar, R. Goumont, F. Terrier, *J. Org. Chem.* **2006**, *71*, 5527–5537.
[22] C. Boga, E. Del Vecchio, L. Forlani, R. Goumont, F. Terrier, S. Tozzi, *Chem. Eur. J.* **2007**, *13*, 9600–9607.
[23] G. Ya. Remmenikov, B. Kempf, A. R. Ofial, K. Polborn, H. Mayr, *J. Phys. Org. Chem.* **2003**, *16*, 431–437.
[24] S. V. Kurbatov, A. V. Tatarov, V. I. Minkin, R. Goumont, F. Terrier, *Chem. Commun.* **2006**, 4279–4281.
[25] L. P. Olekhnovich, Z. N. Budarina, A. V. Lesin, S. V. Kurbatov, G. S. Borodkin, V. I. Minkin, *Mendeleev Commun.* **1994**, 162–163.
[26] F. Terrier, M. Sebban, R. Goumont, J. C. Hallé, G. Moutiers, J. Cangelosi, E. Buncel, *J. Org. Chem.* **2000**, *65*, 7391–7398.
[27] F. Terrier, S. Lakhdar, T. Boubaker, R. Goumont, *J. Org. Chem.* **2005**, *70*, 6242–6253.
[28] M. A. K. Sikder, R. B. Salunke, N. Sikder, *J. Energ. Mat.* **2001**, *25*, 1549–1552.
[29] M. Bemi, M. Vasilescu, M. T. Caproiu, C. Draghici, A. Beteringhe, T. Constantinescu, M. D. Banciu, A. T. Balaban, *Cent. Eur. J. Chem.* **2004**, 672–685.
[30] A. Nemeikaité-Ceniene, J. Sarlauskas, L. Miseviciene, Z. Anusevicius, A. Maroziene, N. Cenas, *Acta Biochem. Pol.* **2004**, *51*, 1081–1086.
[31] M. I. Evgen'yev, S. Y. Garmonov, M. I. Evgen'yeva, L. S. Gazizullina, *J. Anal. Chem.* **1998**, *53*, 571–574.
[32] M. I. Evgen'yev, S. Y. Garmonov, M. I. Evgen'yeva, S. M. Goryunova, V. I. Pogorel'tsev, F. S. Levinson, *Talanta*, **1998**, *47*, 891–898.
[33] M. I. Evgen'ev, I. I. Evgen'eva, F. S. Levinson, E. A. Ermolaeva, Ya. R. Valitova, *Zh. Anal. Khim.* **2006**, *61*, 143–148.
[34] S. Lakhdar, R. Goumont, T. Boubaker, M. Mokhtari, F. Terrier, *Org. Biomol. Chem.* **2006**, *4*, 1910–1919.
[35] J. C. Hallé, D. Vichard, M. J. Pouet, F. Terrier, *J. Org. Chem.* **1997**, *62*, 7178–7182.
[36] D. Vichard, J. C. Hallé, B. Huguet, M. J. Pouet, D. Riou, F. Terrier, *Chem. Commun.* **1998**, 791–792.
[37] P. Sepulcri, J. C. Hallé, R. Goumont, D. Riou, F. Terrier, *J. Org. Chem.* **1999**, *64*, 9254–9257.
[38] R. Goumont, M. Sebban, P. Sepulcri, J. Marrot, F. Terrier, *Tetrahedron* **2002**, *58*, 3249–3262.
[39] G. Kresze, H. Bathelt, *Tetrahedron* **1973**, *29*, 1043–1045.
[40] S. E. Denmark, A. Thorarensen, *Chem. Rev.* **1996**, *96*, 137 and references cited therein. **1996**, *96*, 137–166.
[41] S. E. Denmark, J. A. Dixon, *J. Org. Chem.* **1998**, *63*, 6167–6177.
[42] D. B. Boger, S. N. Weinreb, in *Hetero Diels-Alder Methodology in Organic Synthesis*, Academic Press, New York, **1987**, 71–93.
[43] P. Arroyo, M. T. Picher, L. R. Domingo, *J. Mol. Struct.* **2004**, *709*, 45–52.
[44] P. Arroyo, M. T. Picher, L. R. Domingo, F. Terrier, *Tetrahedron* **2005**, *61*, 7359–7365.
[45] S. Kurbatov, R. Goumont, J. Marrot, F. Terrier, *Tet. Lett.* **2004**, *45*, 1037–1041.
[46] S. Kurbatov, R. Goumont, S. Lahkdar, J. Marrot, F. Terrier, *Tetrahedron*, **2005**, *61*, 8167–8176.
[47] G. Parr, L. von Szentpaly, S. Liu, *J. Am. Chem. Soc.* **1999**, *121*, 1922–1924.
[48] A. D. Becke, *J. Chem. Phys.* **1993**, *98*, 5648–5652.
[49] C. Lee, W. Yang, R. G. Parr, *Phys. Rev. B* **1988**, *37*, 785–789.
[50] W. J. Hehre, L. Radom, Pv. R. Schleyer, J. A. Pople, in *Ab Initio Molecular Orbital Theory*, Wiley, New York, **1986**.
[51] H. B. Schlegel, *J. Comput. Chem.* **1982**, *3*, 214–218.
[52] H. B. Schlegel, in *Modern Electronic Structure Theory*, (Ed.: D. R. Yarkony), World Scientific Publishing, Singapore, **1994**.

[53] R. M. Minyaev, *Russ. Chem. Rev.* **1994**, *11*, 939–961.
[54] A. E. Reed, R. B. Weinstock, F. Weinhold, *J. Chem. Phys.* **1985**, *83*, 735–746.
[55] A. E. Reed, L. A. Curtiss, F. Weinhold, *Chem. Rev.* **1988**, *88*, 899–926.
[56] B. Ya. Simkin, I. I. Sheikhet, in *Quantum Chemical and Statistical Theory of Solutions: A Computational Approach*, Ellis Harwood, London, **1995**.
[57] E. Cances, B. Mennucci, J. Tomasi, *J. Chem. Phys.* **1997**, *107*, 3032–3041.
[58] M. Cossi, V. Barone, R. Cammi, J. Tomasi, *J. Chem. Phys. Lett.* **1996**, *255*, 327–335.
[59] V. Barone, M. Cossi, J. Tomasi, *J. Comput. Chem.* **1998**, *19*, 404–417.
[60] M. J. Frisch, G. W. Trucks, H. B. Schlegel, G. E. Scuseria, M. A. Robb, J. R. Cheeseman, J. A. Montgomery, Jr, T. Vreven, K. N. Kudin, J. C. Burant, J. M. Millam, S. S. Iyengar, J. Tomasi, V. Barone, B. Mennucci, M. Cossi, G. Scalmani, N. Rega, G. A. Petersson, H. Nakatsuji, M. Hada, M. Ehara, K. Toyota, R. Fukuda, J. Hasegawa, M. Ishida, T. Nakajima, Y. Honda, O. Kitao, H. Nakai, M. Klene, X. Li, J. E. Knox, H. P. Hratchian, J. B. Cross, V. Bakken, C. Adamo, J. Jaramillo, R. Gomperts, R. E. Stratmann, O. Yazyev, A. J. Austin, R. Cammi, C. Pomelli, J. W. Ochterski, P. Y. Ayala, K. Morokuma, G. A. Voth, P. Salvador, J. J. Dannenberg, V. G. Zakrzewski, S. Dapprich, A. D. Daniels, M. C. Strain, O. Farkas, D. K. Malick, A. D. Rabuck, K. Raghavachari, J. B. Foresman, J. V. Ortiz, Q. Cui, A. G. Baboul, S. Clifford, J. Cioslowski, B. B. Stefanov, G. Liu, A. Liashenko, P. Piskorz, I. Komaromi, R. L. Martin, D. J. Fox, T. Keith, M. A. Al-Laham, C. Y. Peng, A. Nanayakkara, M. Challacombe, P. M. W. Gill, B. Johnson, W. Chen, M. W. Wong, C. Gonzalez, J. A. Pople, *Gaussian-03, Revision B.04,* Gaussian, Inc., Pittsburgh PA, **2003**.
[61] L. R. Domingo, M. J. Aurell, P. Perez, R. Contreras, *Tetrahedron* **2002**, *58*, 4417–4423.
[62] L. R. Domingo, M. J. Aurell, P. Perez, R. Contreras, *Tetrahedron* **2003**, *59*, 3117–3125.
[63] L. R. Domingo, M. J. Aurell, P. Perez, R. Contreras, *J. Phys. Chem. A* **2002**, *106*, 6871–6875.
[64] R. G. Parr, W. Yang, in *Density Funtional Theory of Atoms and Molecules*, Oxford University Press, New York, **1989**.
[65] R. G. Parr, R. G. Pearson, *J. Am. Chem. Soc.* **1983**, *105*, 7512–7516.
[66] L. R. Domingo, P. Perez, R. Contreras, *Tetrahedron* **2004**, *60*, 6585–6591.
[67] S. Lakhdar, R. Goumont, G. Berionni, T. Boubaker, S. Kurbatov, F. Terrier, *Chem. Eur. J.* **2007**, *13*, 8317–8324.
[68] L. R. Domingo, A. Asensio, P. Arroyo, *J. Phys. Org. Chem.* **2002**, *15*, 660–666.
[69] W. Zhuang, R. G. Hazell, K. A. Jørgensen, *Org. Biomol. Chem.* **2005**, *3*, 2566–2571.
[70] M. Bandini, A. Garelli, M. Rovinetti, S. Tommasi, A. Umani-Ronchi, *Chirality* **2005**, *17*, 522–529.
[71] S. F. Lu, D.-M. Du, J. Xu, *Org. Lett.* **2006**, *8*, 2115–2118.
[72] Y.-X. Jia, S.-F. Zhu, Y. Yang, Q. L. Zhou, *J. Org. Chem.* **2006**, *71*, 75–80.
[73] K. B. Jensen, J. Thorhauge, R. G. Hazell, K. A. Jørgensen, *Angew. Chem. Int. Ed.* **2001**, *113*, 160–163.
[74] J. Zhou, Y. Tang, *J. Am. Chem. Soc.* **2002**, *124*, 9030–9031.
[75] N. R. Kestner, *Rev. Comput. Chem.* **1999**, *13*, 99–132.
[76] F. B. van Duijneveldt, in *Molecular Interactions* (Ed.: S. Scheiner), Wiley, New York, **1997**.
[77] A. S. Bailey, J. R. Case, *Tetrahedron* **1958**, *3*, 113–131.

